

Post-AGB Stars as Tracers of AGB Nucleosynthesis: An Update

Devika Kamath ^{1,2,*}  and Hans Van Winckel ^{3,*} ¹ Department of Physics and Astronomy, Macquarie University, Sydney, NSW 2118, Australia² Astronomy, Astrophysics and Astrophotonics Research Centre, Macquarie University, Sydney, NSW 2118, Australia³ Institute of Astronomy, K.U.Leuven, Celestijnenlaan 200D bus 2401, B-3001 Leuven, Belgium

* Correspondence: devika.kamath@mq.edu.au (D.K.); hans.vanwinckel@kuleuven.be (H.V.W.)

Abstract: The chemical evolution of galaxies is governed by the chemical yields from stars, and here we focus on the important contributions from asymptotic giant branch (AGB) stars. AGB nucleosynthesis is, however, still riddled with complexities. Observations from post-asymptotic giant branch (post-AGB) stars serve as exquisite tools to quantify and understand AGB nucleosynthesis. In this contribution, we review the invaluable constraints provided by post-AGB stars with which to study AGB nucleosynthesis, especially the slow neutron capture nucleosynthesis (i.e., the *s*-process).

Keywords: stars: AGB and post-AGB; stars: chemically peculiar; neutron-capture processes; Magellanic clouds; Galaxy: stellar content; stars: abundances; techniques: spectroscopy

1. Introduction

To answer part of the long-standing yet significant question in Astrophysics, “How are elements in the Universe formed?” we focus on low- and intermediate-mass (LIM) stars, i.e., those with masses of ~ 1 to 8 times that of our Sun. LIM stars in their asymptotic giant branch (AGB) phases of evolution are estimated to produce $\sim 90\%$ of the solid material injected into the interstellar medium [1], and are known to be one of the major producers of elements such as carbon, nitrogen and about half of the elements heavier than iron [2]: AGB stars are clearly key contributors to the chemical enrichment of the Universe.

For low- and intermediate-mass stars (i.e., those with masses of ~ 1 to 8 times that of our Sun), it is in the AGB phase where we expect the largest changes to their surface composition. During the AGB phase, the photospheric abundance pattern of the object is altered in two ways. Firstly, by third dredge-up (TDU) episodes [3–5] wherein the elements and isotopes that are freshly synthesised within the star are brought to the surface through convection-driven mixing processes. These processes are responsible for enriching the stellar photosphere with products of internal nucleosynthesis, such as carbon (C), nitrogen (N) and oxygen (O), and converting stars into carbon-rich (C-rich) stars with a C/O ratio greater than unity [5]. These mixing processes are also responsible for fuelling the synthesis of, and subsequently enriching the stellar surface with, elements heavier than iron (Fe), such as strontium (Sr), zirconium (Zr), barium (Ba), lanthanum (La), lead (Pb) and elements in between. These heavy elements are thought to be produced by the addition of neutrons onto Fe and other elements, wherein the neutron capture is slow with respect to the competing β^- decay. This mechanism, which occurs deep in the stellar interior, is referred to as the slow neutron capture process (*s*-process, e.g., [6,7]). To be able to reproduce the observed *s*-process abundances in the Sun, it was realised that the *s*-process could not entirely take place in one single astrophysical site. Therefore, historically, the *s*-process has been separated into three components, each of which has its own mean value of time-integrated neutron flux, or neutron exposure (τ) [8], which is typically expressed in mbarn^{-1} . Each component is linked to a specific astrophysical site. The weak component produces nuclei with mass numbers (*A*) ranging from $56 < A \leq 90$, the Sr-peak, and has



Citation: Kamath, D.; Van Winckel, H. Post-AGB Stars as Tracers of AGB Nucleosynthesis: An Update. *Universe* **2022**, *8*, 233. <https://doi.org/10.3390/universe8040233>

Academic Editor: Sara Palmerini

Received: 25 January 2022

Accepted: 27 March 2022

Published: 11 April 2022

Publisher's Note: MDPI stays neutral with regard to jurisdictional claims in published maps and institutional affiliations.



Copyright: © 2022 by the authors. Licensee MDPI, Basel, Switzerland. This article is an open access article distributed under the terms and conditions of the Creative Commons Attribution (CC BY) license (<https://creativecommons.org/licenses/by/4.0/>).

a typical $\tau \approx 0.07 \text{ mbarn}^{-1}$ [9]. The main component produces nuclei with $90 \leq A \leq 204$, the mean of which is $\tau \approx 0.3 \text{ mbarn}^{-1}$, and the strong component, with a neutron exposure of $\tau \approx 7.0 \text{ mbarn}^{-1}$, produces nuclei with $A = 204$ to 208, i.e., up to to ^{208}Pb . The weak component is thought to be mainly produced in the He- and C-burning shells of massive stars (e.g., [10]), the main component occurs in low-mass AGB stars (e.g., [4]) and the strong component is produced in low-mass, metal-deficient AGB stars (e.g., [11]). The strong component mainly exists out of ^{208}Pb , which is a nucleus with both neutron and proton counts equal to a magic number and is therefore called “double magic”. This implies that ^{208}Pb is very stable against decay and has a very small cross-section for neutron capture, marking it as the end-product of the *s*-process chain.

Secondly, by hot bottom burning (HBB), which is predicted to be active only in stars with initial masses greater than $\sim 2.5 M_{\odot}$ (depending on the metallicity and the input physics of the stellar model). HBB prevents the formation of C-rich photospheres by burning ^{12}C into ^{14}N [7,12,13]. There is strong evidence that some of the ^{14}N in the universe is of primary origin [14], which comes from AGB stars. AGB models also suggest that HBB in AGB stars may also involve the Ne–Na and Mg–Al chains, leading to changes in the surface abundances of Na, Mg and Al (see [7,13] and references therein).

In this study, we succinctly review the role of post-asymptotic giant branch (post-AGB) stars as tracers of AGB nucleosynthesis and present the latest observational and theoretical developments in this research landscape.

2. Post-AGB Stars—Exquisite Tracers of AGB Nucleosynthesis

While AGB stars can be used to quantify isotopic ratios of carbon (C) and oxygen (O), and those of elements such as zirconium (Zr) and rubidium (Rb) (e.g., [15,16]), they pose challenges, since their spectra are veiled by molecular lines [17] and modelling of their dynamical atmospheres is rather complex and uncertain [18].

Post-AGB stars, the progeny of AGB stars, contain the products of AGB nucleosynthesis. During the brief post-AGB phase, the warm stellar photosphere makes it possible to quantify photospheric abundances for a very wide range of elements, including C, N, O and the heaviest *s*-process elements [19] that are brought to the stellar surface during the AGB phase. This makes post-AGB stars ideal tracers of AGB nucleosynthesis.

At the very end of the AGB phase, stars lose mass via a powerful wind, driven by stellar pulsations [20] or by interaction with another star for stars in binary systems [21,22]. This sheds the entire outer envelope, and for an astronomically brief moment ($< 10,000$ years)—referred to as the post-AGB phase—the chemically enriched surface of the star is exposed [23]. This makes post-AGB stars formidable probes to examine the elements produced by the star during and prior to the AGB phase (e.g., [24–28]).

The post-AGB phase of evolution is a transient phase between the AGB and planetary nebula (PN) phases of stellar evolution. During the AGB phase, a super-wind with mass-loss rates up to $10^{-4} M_{\odot} \text{ year}^{-1}$ reduces the mass of the hydrogen envelope to $\sim 0.02 M_{\odot}$, thereby terminating the AGB phase of evolution. Subsequently, the radius of the central star decreases, and within about 10^2 – 10^4 years, the star evolves to higher temperatures (from 3×10^3 K on the AGB to $\sim 3 \times 10^4$ K with a constant luminosity (e.g., [20,29,30]). The ejected circumstellar matter expands and cools during the post-AGB phase, resulting in stars with large mid-IR excess (see [23,31,32] for reviews). Post-AGB stars emit radiation that spans the UV, optical and IR spectral regime, owing to a combination of high temperatures in the photosphere and low temperatures in circumstellar dust. This enables the simultaneous study of the stellar photosphere and the circumstellar environment: the central star emits in the ultra-violet (UV), optical and near-infrared (IR) bands, and the cool circumstellar environment radiates in the near- and mid-IR bands. As the post-AGB star evolves to higher temperatures, the ejected circumstellar material gets ionised to form a PN. Subsequently, the central star ends its nucleosynthetic energy production. The central star is first a hot white dwarf which cools on the white dwarf cooling tracks (e.g., [33]). Signatures of chemical

enrichment are lost in this process. Therefore, post-AGB stars are truly cosmic treasures and exquisite probes of AGB nucleosynthesis.

For stars in binary systems, a different mechanism can terminate the red giant evolution (see [21,22]). The large expansion that occurs when a star becomes a red giant can cause the primary star to over-fill its Roche lobe. Theory suggests that Roche lobe overflow during the red giant phase will lead to run-away mass transfer on a dynamical or thermal timescale, until all that is left of the mass-losing star is the He or C/O core of the red giant, orbiting in a binary system; alternatively, complete merging may occur (e.g., [34–36]). This process occurs for binaries with periods on the main sequence ranging from 20 to 1000 days, from low on the red giant branch (RGB) to the tip of the AGB. The outcomes of these systems are as of yet difficult to predict, as many binary interaction processes are poorly understood. A significant fraction of the ejected matter may end up in a circumbinary disc of dust and gas, and inside the disc is a binary system containing a post-AGB star (see [37] and references therein).

One of the challenges in the study of the post-AGB phase of evolution is the identification of post-AGB objects, as they have very short lifetimes. Since they have dusty circumstellar envelopes, the detection of cold circumstellar dust using mid-IR photometry is an efficient method to select and study them. The first extensive search for these objects was initiated in the mid-80s using results from the Infrared Astronomical Satellite (IRAS). The large scale mid-IR IRAS mission enabled the identification of post-AGB stars in the Galaxy [31]. The Toruń catalogue [38] for Galactic post-AGB stars lists around 391 very likely post-AGB objects. The Galactic sample of optically visible post-AGB objects has revealed two highly distinct populations: one with cold, detached, expanding dust shells and another with hot dust and circumstellar discs (see Figure 1). The former probably arise from single stars and produce “shell” or “outflow sources” [23]. The latter arise from binary stars and are called “disc sources” [39–43].

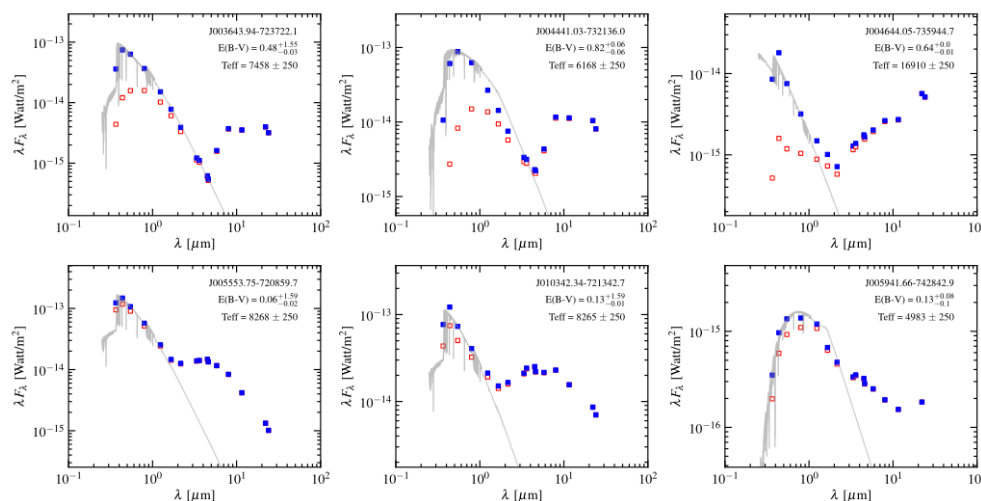


Figure 1. Sample spectral energy distributions (SEDs) of post-AGB stars. The top row represents examples of shell-type SEDs, typical for single stars. The bottom row represents examples of disc-type SEDs, typical for binary post-AGB stars with circumbinary disks. Figure adapted from [44].

Previously, in the Galaxy, the luminosities (and hence initial masses) of the diverse group of post-AGB stars were highly uncertain because of their poorly constrained distances, making it difficult to use the observational characteristics of these interesting objects to throw light on the poorly-understood late stages of stellar evolution. In our recent study [45], we exploited the *Gaia* Early Data Release 3 (*Gaia* EDR3), which provided the opportunity to obtain accurate distances and hence luminosities for the sample of known single post-AGB stars in our Galaxy.

In our past studies, we have also focused on the Magellanic clouds [22,44,46,47]. The well-constrained distances to these extragalactic systems mean that distance-dependent parameters, such as luminosities, can be determined accurately. The large magellanic cloud (LMC) and small magellanic cloud (SMC) are both very suitable environments within which to locate individual post-AGB objects and study their evolution as a function of initial mass and metallicity.

To date, chemical abundance studies of post-AGB stars in the Galaxy, LMC and SMC (see [27,28,45] and references therein) have shown an intriguing chemical diversity that ranges from stars that are extremely enriched in carbon and *s*-process elements [25,26,45] to the discovery of the first post-AGB star with no traces of carbon nor *s*-process elements [45,48]. Additionally, stellar nucleosynthesis is significantly affected by a binary companion [43,49,50]. These results reflect the complexity that surrounds the element production in AGB stars. In this contribution, we mainly focus on the current research landscape of using post-AGB stars as tracers of *s*-process nucleosynthesis.

3. The *s*-Process in Post-AGB Stars

In this section, we give a short overview on the chemical abundances of post-AGB stars and point to several papers where the interested readers can find more details on the specific abundance distributions. In our overview we focus on primarily the *s*-process elements.

The *s*-process was traditionally studied in extrinsic stars (e.g., Ba stars, CH stars and CEMP-*s* stars), where the visible object is the companion which is polluted or enriched by *s*-process-rich material from its former AGB companion, which is now typically a dim white dwarf. However, in these extrinsic stars, the properties of the polluting AGB star and the associated AGB nucleosynthetic processes are difficult to determine. *s*-process-rich post-AGB stars, the direct progeny of AGB stars, are intrinsically enriched with products of AGB nucleosynthesis.

3.1. Galaxy

The first studies focusing on the *s*-process elemental abundances started with individual studies of isolated Galactic objects (e.g., [51,52]). Many authors followed, and overview papers on the results of these abundance determinations of Galactic sources can be found in, e.g., [19,23,53–55] and references therein.

Some post-AGB stars are the most *s*-process-rich objects we know. This provides means to study elements even beyond the Ba peak. This was illustrated by [19], who systematically studied the most *s*-process-rich objects in their study of Gd, Yb, Lu and W abundances. The sensitivity of hyperfine splitting of elements such as Lu makes the quantified abundance determinations challenging.

The end product of the *s*-process is in the double magic Pb. Pb does, however, not have a rich spectrum in the optical band, and depending on the effective temperature of the star, the strongest Pb line is either Pb I at λ 4057.807 or the Pb II line at λ 5608.854 . The first especially is in a very dense region of the optical domain, making positive detections difficult [55]. To our knowledge, we only know upper-limits of the Pb abundances in Galactic post-AGB stars, as we do not have clear detections of these lines.

Interesting to note is that the most *s*-process-rich objects are associated with what is called the 21 μ m sources. This dust feature was originally discovered back in 1989 [56] in the circumstellar dust of some carbon-rich post-AGB stars. The true chemical nature of the 21 μ m dust feature remains illusive, and a recent review can be found in [57]. The feature is transient and is not observed in AGB stars, nor in PNe, but only in post-AGB stars with a limited range of effective temperatures. The feature is associated with carbon-rich environments and illustrated the connection between carbon enhancement and the increase in the *s*-process elements. Given that the 21 μ m dust feature remains enigmatic, it is fair to say that we do not yet have a full, self consistent chemical evolution model which connects the atmospheric abundances to the circumstellar dust and gas envelope.

3.2. Magellanic Clouds

The first identification of post-AGB stars in the LMC and SMC was made possible using the sample of high-luminosity population II Cepheids that was discovered through the gravitational lens experiment MACHO [58]. The first *s*-process-rich magellanic-cloud post-AGB star was identified from this target sample (i.e., MACHO 47.2496.8 [49]).

A more systematic search for post-AGB stars became possible with the infrared point-source data of the Spitzer-SAGE experiment of the LMC [59] and the SMC [60,61]. These Spitzer Space Telescope surveys allowed for the initial selection of candidates with large mid-IR excess—the characteristic of post-AGB stars. Subsequently, low-resolution optical spectroscopic surveys allowed for the identification of optically bright post-AGB stars. The dedicated spectroscopic searches of post-AGB stars in the LMC [46,47] and in the SMC [44] revealed many good candidates for high-resolution spectral follow-up.

Using 8 m class telescopes, high-resolution spectra of LMC and SMC post-AGB objects were obtained. Similarly to the Galactic post-AGB star studies, detailed chemical abundance studies revealed extremely *s*-process-enriched objects in the LMC and the SMC [24–26].

3.3. An Example of an Extremely Enriched SMC Object: J004441.04-732136.4

To illustrate the impact of *s*-process enhancements in post-AGB stars, we highlight the SMC object J004441.04-732136.4 (see Figures 2 and 3). The spectra are dominated by lines of *s*-process elements, including trace elements such as neodymium (Nd), praseodymium (Pr) and La. This is illustrated in Figures 2 and 3. These figures show small spectral windows of three stars with similar temperatures and metallicity, but only the bottom two stars are *s*-process-rich.

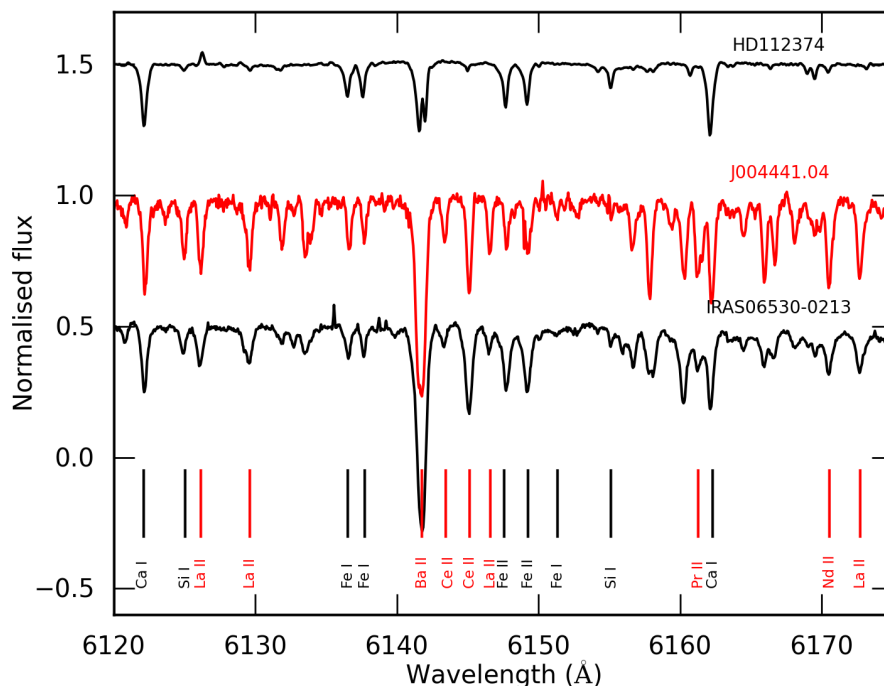


Figure 2. Spectral comparison of three stars with similar temperatures and overall metallicity. Only the top spectrum is from a star without *s*-process enhancements. In very enriched objects, the *s*-process lines almost dominate the spectral appearance. Figure from [24].

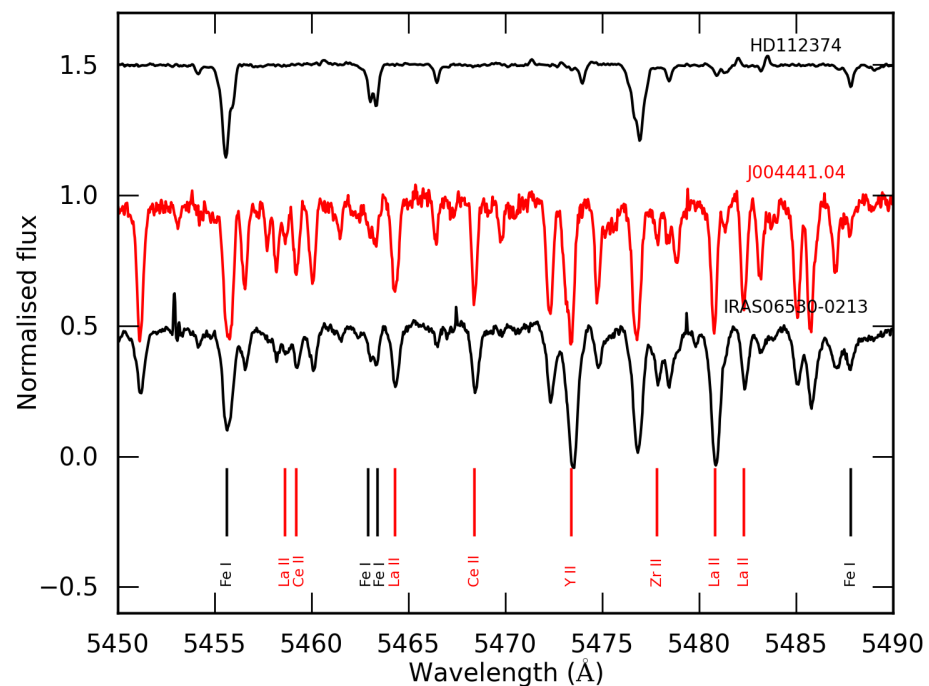


Figure 3. Spectral comparison of three stars with similar temperatures and overall metallicity. Only the top spectrum is from a star without *s*-process enhancements. In very enriched objects (i.e., the bottom two spectra), the *s*-process lines almost dominate the spectral appearance. Figure from [24].

Owing to the richness in atomic lines, spectra of *s*-process-rich post-AGB stars lead to the identification of several *s*-process lines [62]. However, several spectral lines in the optical remain unidentified (e.g., [24] and line identification in these very *s*-process-rich environments is often still a challenge.

4. The *s*-Process in Post-AGB Stars: The Observational Findings

With overabundances reaching [*s*-process/Fe] of ~ 3 dex, some post-AGB stars are among the most *s*-process-enriched objects known to date.

4.1. [*hs*/*ls*] versus [*Fe*/*H*] Relation

As the neutron source in low-mass AGB stars is believed to come from the ^{13}C -pocket, made via proton capture on the freshly made (primary) ^{12}C , the neutron source is thought to be largely independent of the initial metallicity. For low metallicity environments, there are more neutrons available per iron-seed, and the neutron irradiation is predicted to be higher (e.g., [4,6,7,63,64].

The ratio between the barium-peak elements (*hs*) and the strontium-peak elements (*ls*) is widely used as a good measure for the neutron exposure. Models predict a correlation between neutron exposure and metallicity. In Figure 4, we illustrate that this correlation does not exist in the metallicity range as covered by *s*-process-rich post-AGB stars.

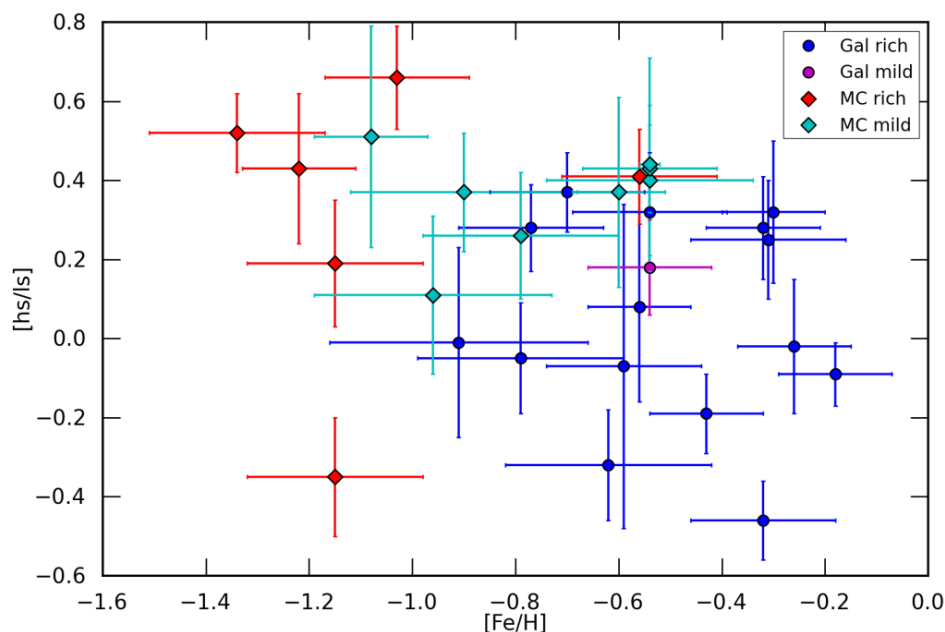


Figure 4. $[\text{Fe}/\text{H}]$ versus $[\text{hs}/\text{ls}]$. Within the metallicity range covered by the s -process-rich post-AGB stars, there is no correlation between neutron exposure, as depicted in the $[\text{hs}/\text{ls}]$ ratio, and intrinsic metallicity—for the Galaxy and for the LMC/SMC. Figure from [65].

4.2. The Lead Problem

Pb is the end-product of the s -process chain. At low metallicities, AGB models predict high Pb abundances. Post-AGB stars provide an interesting metallicity range which is higher than that of the metal-poor CEMP stars, to test the production of Pb and thereby the s -process nucleosynthesis.

High Pb abundances have been detected in some but not all CEMP-s stars (e.g., [66,67]). However, in post-AGB stars, Pb is not detected. The observationally derived Pb upper limits are significantly lower than what are predicted by models [55]. We refer to [28] for a full description of what we call the Pb problem. This is likely linked to the lack of correlation between the hs/ls ratio and metallicity.

4.3. The i -Process

Within the heavy element nucleosynthesis, two different regimes in neutron exposure are historically defined: the s -process or slow neutron capture process, which follows closely the valley of stability during successive neutron captures, and the r -process (a rapid process), defined as an exposure at very high neutron densities and during which isotopes far from the valley of stability are formed. These will decay towards the neutron-rich part of the valley of stability.

Recently, however, several observational constraints from the distribution of heavy elements observed in, e.g., CEMP-stars, but also post-AGB stars, lead to the proposition of an i -process, which stands for “intermediate” process, with an exposure to neutron densities in between the s and r -processes. This was introduced back in 1977 [68], but the discussion on the i -process gained strong momentum in recent years when more and more abundance determinations became available. The discussion on the i -process is focussed on CEMP-rs stars which show overabundances of both typical s -process isotopes and typical r -process elements (e.g., [69–71]).

While a review on the i -process is beyond the scope of this paper, both the Pb problem and the presence of a wide variety of neutron exposures within the post-AGB sample are indicative of the presence of irradiation at intermediate neutron densities (e.g., [55,72]). For a more elaborate discussion on the i -process within post-AGB stars, we refer to [28].

4.4. $[s/H]$ versus $[Fe/H]$ Relation: The Haves and Have-Not

As mentioned in Section 2, an intriguing puzzle yet to be solved is the chemical diversity observed in post-AGB stars, especially among the single stars. Post-AGB single stars, in the Galaxy, with seemingly very similar stellar properties, display a wide range of s -process overabundances. This is illustrated in Figure 5, where s -process enrichments are displayed against metallicity. There is a bifurcation such that some post-AGB atmospheres are very enriched in s -process elements (previously referred to as “haves”) while others (i.e., the have-nots) are not s -process-enriched at all [23]. This bi-modality was initially attributed to a likely initial-mass affect; however, previously poorly constrained distances and hence luminosities made it difficult confirm the same.

The release of the *Gaia* EDR3 catalogue made it possible for us to determine accurate distances (and hence luminosities) to the Galactic post-AGB single star sample and constrain their positions in the HR diagram [45]. Our study has revealed that the two classes of objects do not show any distinct difference in luminosity (and hence initial mass). Therefore, it is likely that other factors besides initial-mass and metallicity affect AGB nucleosynthesis.

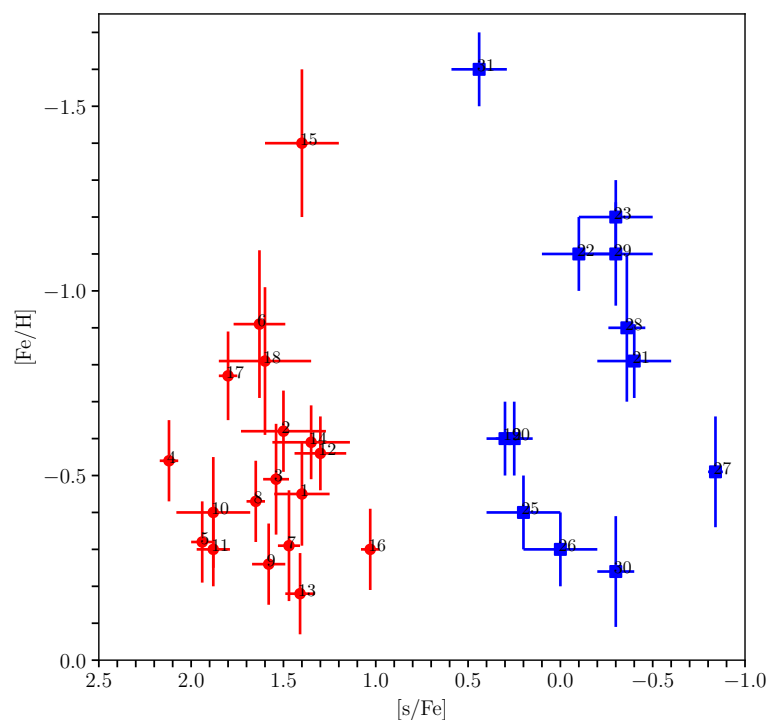


Figure 5. $[s/Fe]$ versus metallicity. Within the post-AGB sample of Galactic, LMC and SMC stars, there is a wide variety of s -process enrichment which is independent of stellar metallicity. Many non-enriched objects which failed the third dredge-up are present as well. Figure adapted from [45]. The numbers in the figure refer to specific objects, as reviewed in [45].

The discovery of post-AGB stars in the LMC and SMC (where the distances and hence luminosities and initial-masses are well constrained) has revealed that the chemical diversity observed in Galactic post-AGB stars is also present within the SMC and LMC sample [48].

5. Conclusions

Optically bright post-AGB stars with their spectra dominated by atomic transitions provide unique constraints on AGB nucleosynthesis. We reviewed the most important findings from the abundance studies in the literature and isolated several challenges due to the chemical diversity detected among post-AGB stars being in contrast with the model predictions.

The observational astrophysical endeavour is far from finished. In particular, many of the post-AGB stars found in the LMC and SMC remain to be studied with high S/N and high-resolution spectroscopy. Moreover, the full *Gaia* DR3 (to be released in June 2022) will lead to much better constraints on the luminosities of the Galactic sample, which means that in the near future, chemical abundance studies of a more comprehensive sample of post-AGB stars will become available.

The chemical diversity currently observed in post-AGB stars (e.g., [27,45]) reflects the complexity of AGB nucleosynthesis. Open questions include the true nature of the convective and non-convective mixing mechanisms, the nature of the neutron-capture processes operating in AGB stars and also the true neutron production sites in AGB stars. More recent theoretical developments can be found in (e.g., [73,74]), which complement the observational research carried out on post-AGB stars.

Author Contributions: D.K. and H.V.W. contributed substantially to the conceptualisation, composition, editing and revision of this manuscript. All authors have read and agreed to the published version of the manuscript.

Funding: D.K. acknowledges support from the Australian Research Council through DECRA grant number DE190100813. This research was supported in part by the Australian Research Council Centre of Excellence for All Sky Astrophysics in 3 Dimensions (ASTRO 3D) through project number CE170100013. H.V.W. acknowledges support from the Research Council of the KU Leuven under grant number C14/17/082.

Institutional Review Board Statement: Not applicable.

Informed Consent Statement: Not applicable.

Data Availability Statement: Not applicable.

Acknowledgments: DK acknowledges support from the Australian Research Council through DECRA grant number DE190100813. This research was supported in part by the Australian Research Council Centre of Excellence for All Sky Astrophysics in 3 Dimensions (ASTRO 3D) through project number CE170100013. HVW acknowledges support from the Research Council of the KU Leuven under grant number C14/17/082.

Conflicts of Interest: The authors declare no conflict of interest.

References

1. Sloan, G.C.; Kraemer, K.E.; Wood, P.R.; Zijlstra, A.A.; Bernard-Salas, J.; Devost, D.; Houck, J.R. The Magellanic Zoo: Mid-Infrared Spitzer Spectroscopy of Evolved Stars and Circumstellar Dust in the Magellanic Clouds. *Astrophys. J.* **2008**, *686*, 1056–1081. [[CrossRef](#)]
2. Kobayashi, C.; Karakas, A.I.; Lugaro, M. The origin of elements from carbon to uranium. *Astrophys. J.* **2020**, *900*, 179. [[CrossRef](#)]
3. Iben, I., Jr.; Renzini, A. Asymptotic giant branch evolution and beyond. *Annu. Rev. Astron. Astrophys.* **1983**, *21*, 271–342. [[CrossRef](#)]
4. Busso, M.; Gallino, R.; Wasserburg, G.J. Nucleosynthesis in Asymptotic Giant Branch Stars: Relevance for Galactic Enrichment and Solar System Formation. *Annu. Rev. Astron. Astrophys.* **1999**, *37*, 239–309. [[CrossRef](#)]
5. Herwig, F. Evolution of Asymptotic Giant Branch Stars. *Annu. Rev. Astron. Astrophys.* **2005**, *43*, 435–479. [[CrossRef](#)]
6. Gallino, R.; Arlandini, C.; Busso, M.; Lugaro, M.; Travaglio, C.; Straniero, O.; Chieffi, A.; Limongi, M. Evolution and Nucleosynthesis in Low-Mass Asymptotic Giant Branch Stars. II. Neutron Capture and the *s*-Process. *Astrophys. J.* **1998**, *497*, 388. [[CrossRef](#)]
7. Karakas, A.I.; Lattanzio, J.C. The Dawes Review 2: Nucleosynthesis and Stellar Yields of Low- and Intermediate-Mass Single Stars. *Publ. Astron. Soc. Aust.* **2014**, *31*, e030. [[CrossRef](#)]
8. Seeger, P.A.; Fowler, W.A.; Clayton, D.D. Nucleosynthesis of Heavy Elements by Neutron Capture. *Astrophys. J.* **1965**, *11*, 121. [[CrossRef](#)]
9. Karakas, A.I. Updated stellar yields from asymptotic giant branch models. *Mon. Not. R. Astron. Soc.* **2010**, *403*, 1413–1425. [[CrossRef](#)]
10. Pignatari, M.; Gallino, R.; Heil, M.; Wiescher, M.; Käppeler, F.; Herwig, F.; Bisterzo, S. The Weak *s*-Process in Massive Stars and its Dependence on the Neutron Capture Cross Sections. *Astrophys. J.* **2010**, *710*, 1557–1577. [[CrossRef](#)]
11. Sneden, C.; Cowan, J.J.; Gallino, R. Neutron-Capture Elements in the Early Galaxy. *Annu. Rev. Astron. Astrophys.* **2008**, *46*, 241–288. [[CrossRef](#)]

12. Boothroyd, A.I.; Sackmann, I.J.; Ahern, S.C. Prevention of High-Luminosity Carbon Stars by Hot Bottom Burning. *Astrophys. J.* **1993**, *416*, 762–768. [[CrossRef](#)]
13. Ventura, P.; Karakas, A.I.; Dell’Agli, F.; Boyer, M.L.; García-Hernández, D.A.; Di Criscienzo, M.; Schneider, R. The Large Magellanic Cloud as a laboratory for hot bottom burning in massive asymptotic giant branch stars. *Mon. Not. R. Astron. Soc.* **2015**, *450*, 3181–3190. [[CrossRef](#)]
14. van Zee, L.; Salzer, J.J.; Haynes, M.P.; O’Donoghue, A.A.; Balonek, T.J. Spectroscopy of Outlying H II Regions in Spiral Galaxies: Abundances and Radial Gradients. *Astron. J.* **1998**, *116*, 2805–2833. [[CrossRef](#)]
15. García-Hernández, D.A.; García-Lario, P.; Plez, B.; Machado, A.; D’Antona, F.; Lub, J.; Habing, H. Lithium and zirconium abundances in massive Galactic O-rich AGB stars. *Astron. Astrophys.* **2007**, *462*, 711–730. [[CrossRef](#)]
16. Hinkle, K.H.; Lebzelter, T.; Straniero, O. Carbon and oxygen isotopic ratios for nearby Miras. *Astrophys. J.* **2016**, *825*, 38. [[CrossRef](#)]
17. Abia, C.; de Laverny, P.; Wahlin, R. Chemical analysis of carbon stars in the Local Group. II. The Carina dwarf spheroidal galaxy. *Astron. Astrophys.* **2008**, *481*, 161–168. [[CrossRef](#)]
18. Pérez-Mesa, V.; Zamora, O.; García-Hernández, D.A.; Osorio, Y.; Masseron, T.; Plez, B.; Machado, A.; Karakas, A.I.; Lugaro, M. Exploring circumstellar effects on the lithium and calcium abundances in massive Galactic O-rich AGB stars. *Astron. Astrophys.* **2019**, *623*, A151. [[CrossRef](#)]
19. Reyniers, M.; Van Winckel, H. Detection of elements beyond the Ba-peak in VLT+UVES spectra of post-AGB stars. *Astron. Astrophys.* **2003**, *408*, L33–L37. [[CrossRef](#)]
20. Vassiliadis, E.; Wood, P.R. Evolution of low- and intermediate-mass stars to the end of the asymptotic giant branch with mass loss. *Astrophys. J.* **1993**, *413*, 641–657. [[CrossRef](#)]
21. Nie, J.D.; Wood, P.R.; Nicholls, C.P. Predicting the fate of binary red giants using the observed sequence E star population: Binary planetary nebula nuclei and post-RGB stars. *Mon. Not. R. Astron. Soc.* **2012**, *423*, 2764–2780. [[CrossRef](#)]
22. Kamath, D.; Wood, P.R.; Van Winckel, H.; Nie, J.D. A newly discovered stellar type: Dusty post-red giant branch stars in the Magellanic Clouds. *Astron. Astrophys.* **2016**, *586*, L5. [[CrossRef](#)]
23. Van Winckel, H. Post-AGB Stars. *Annu. Rev. Astron. Astrophys.* **2003**, *41*, 391–427. [[CrossRef](#)]
24. De Smedt, K.; Van Winckel, H.; Karakas, A.I.; Siess, L.; Goriely, S.; Wood, P.R. Post-AGB stars in the SMC as tracers of stellar evolution: The extreme *s*-Process enrichment of the 21 μm star J004441.04-732136.4. *Astron. Astrophys.* **2012**, *541*, A67. [[CrossRef](#)]
25. De Smedt, K.; Van Winckel, H.; Kamath, D.; Wood, P.R. Chemical abundance study of two strongly *s*-Process enriched post-AGB stars in the LMC: J051213.81-693537.1 and J051848.86-700246.9. *Astron. Astrophys.* **2015**, *583*, A56. [[CrossRef](#)]
26. van Aarle, E.; Van Winckel, H.; De Smedt, K.; Kamath, D.; Wood, P.R. Detailed abundance study of four *s*-Process enriched post-AGB stars in the Large Magellanic Cloud. *Astron. Astrophys.* **2013**, *554*, A106. [[CrossRef](#)]
27. Kamath, D. Post-AGB stars as tracers of the origin of elements in the universe. *J. Astrophys. Astron.* **2020**, *41*, 42. [[CrossRef](#)]
28. Kamath, D.; Van Winckel, H. The Missing Lead: Developments in the Lead (Pb) Discrepancy in Intrinsically *s*-Process Enriched Single Post-AGB Stars. *Universe* **2021**, *7*, 446. [[CrossRef](#)]
29. Schönberner, D. Late stages of stellar evolution. II—Mass loss and the transition of asymptotic giant branch stars into hot remnants. *Astrophys. J.* **1983**, *272*, 708–714. [[CrossRef](#)]
30. Vassiliadis, E.; Wood, P.R. Post-asymptotic giant branch evolution of low- to intermediate-mass stars. *Astrophys. J. Suppl. Ser.* **1994**, *92*, 125–144. [[CrossRef](#)]
31. Kwok, S. Proto-planetary nebulae. *Annu. Rev. Astron. Astrophys.* **1993**, *31*, 63–92. [[CrossRef](#)]
32. Habing, H.J.; Olofsson, H. *Asymptotic Giant Branch Stars*; Springer: Berlin/Heidelberg, Germany, 2003.
33. Renedo, I.; Althaus, L.G.; Miller Bertolami, M.M.; Romero, A.D.; Córscico, A.H.; Rohrmann, R.D.; García-Berro, E. New Cooling Sequences for Old White Dwarfs. *Astrophys. J.* **2010**, *717*, 183–195. [[CrossRef](#)]
34. Paczyński, B.; Sienkiewicz, R. Evolution of Close Binaries VIII. Mass Exchange on the Dynamical Time Scale. *Acta Astron.* **1972**, *22*, 73–91.
35. Iben, I., Jr.; Tutukov, A.V.; Yungelson, L.R. On the Origin of Hydrogen-deficient Supergiants and Their Relation to R Coronae Borealis Stars and Non-DA White Dwarfs. *Astrophys. J.* **1996**, *456*, 750. [[CrossRef](#)]
36. Han, Z.; Podsiadlowski, P.; Eggleton, P.P. The formation of bipolar planetary nebulae and close white dwarf binaries. *Mon. Not. R. Astron. Soc.* **1995**, *272*, 800–820.
37. van Winckel, H. Post-AGB Binaries as Tracers of Stellar Evolution. Planetary Nebulae: Multi-Wavelength Probes of Stellar and Galactic Evolution. *IAU Symp.* **2017**, *12*, 231–234. [[CrossRef](#)]
38. Szczerba, R.; Siódmiak, N.; Stasińska, G.; Borkowski, J. An evolutionary catalogue of galactic post-AGB and related objects. *Astron. Astrophys.* **2007**, *469*, 799–806. [[CrossRef](#)]
39. de Ruyter, S.; Van Winckel, H.; Maas, T.; Lloyd Evans, T.; Waters, L.B.F.M.; Dejonghe, H. Keplerian discs around post-AGB stars: A common phenomenon? *Astron. Astrophys.* **2006**, *448*, 641–653. [[CrossRef](#)]
40. Van Winckel, H. Post-Agb Binaries. *Balt. Astron.* **2007**, *16*, 112–119.
41. Gielen, C.; Van Winckel, H.; Reyniers, M.; Zijlstra, A.; Lloyd Evans, T.; Gordon, K.D.; Kemper, F.; Indebetouw, R.; Marengo, M.; Matsuura, M.; et al. Chemical depletion in the Large Magellanic Cloud: RV Tauri stars and the photospheric feedback from their dusty discs. *Astron. Astrophys.* **2009**, *508*, 1391–1402. [[CrossRef](#)]

42. Van Winckel, H.; Lloyd Evans, T.; Briquet, M.; De Cat, P.; Degroote, P.; De Meester, W.; De Ridder, J.; Deroo, P.; Desmet, M.; Drummond, R.; et al. Post-AGB stars with hot circumstellar dust: Binarity of the low-amplitude pulsators. *Astron. Astrophys.* **2009**, *505*, 1221–1232. [[CrossRef](#)]
43. Oomen, G.M.; Van Winckel, H.; Pols, O.; Nelemans, G.; Escorza, A.; Manick, R.; Kamath, D.; Waelkens, C. Orbital properties of binary post-AGB stars. *Astron. Astrophys.* **2018**, *620*, A85. [[CrossRef](#)]
44. Kamath, D.; Wood, P.R.; Van Winckel, H. Optically visible post-AGB/RGB stars and young stellar objects in the Small Magellanic Cloud: Candidate selection, spectral energy distributions and spectroscopic examination. *Mon. Not. R. Astron. Soc.* **2014**, *439*, 2211–2270. [[CrossRef](#)]
45. Kamath, D.; Van Winckel, H.; Ventura, P.; Mohorian, M.; Hrivnak, B.J.; Dell’Agli, F.; Karakas, A. Luminosities and Masses of Single Galactic Post-asymptotic Giant Branch Stars with Distances from Gaia EDR3: The Revelation of an *s*-Process Diversity. *Astrophys. J.* **2022**, *927*, L13. [[CrossRef](#)]
46. van Aarle, E.; Van Winckel, H.; Lloyd Evans, T.; Ueta, T.; Wood, P.R.; Ginsburg, A.G. The optically bright post-AGB population of the LMC. *Astron. Astrophys.* **2011**, *530*, A90. [[CrossRef](#)]
47. Kamath, D.; Wood, P.R.; Van Winckel, H. Optically visible post-AGB stars, post-RGB stars and young stellar objects in the Large Magellanic Cloud. *Mon. Not. R. Astron. Soc.* **2015**, *454*, 1468–1502. [[CrossRef](#)]
48. Kamath, D.; Van Winckel, H.; Wood, P.R.; Asplund, M.; Karakas, A.I.; Lattanzio, J.C. Discovery of a Metal-poor, Luminous Post-AGB Star that Failed the Third Dredge-up. *Astrophys. J.* **2017**, *836*, 15. [[CrossRef](#)]
49. Reyniers, M.; van Winckel, H. First detection of photospheric depletion in the Large Magellanic Cloud. *Astron. Astrophys.* **2007**, *463*, L1–L4. [[CrossRef](#)]
50. Kamath, D.; Van Winckel, H. Extrinsically metal-poor stars: Photospheric chemical depletion in post-AGB/post-RGB stars in the Large Magellanic Cloud. *Mon. Not. R. Astron. Soc.* **2019**, *486*, 3524–3536. [[CrossRef](#)]
51. Klochkova, V.G. Spectroscopy of F supergiants with infrared excess. *Mon. Not. R. Astron. Soc.* **1995**, *272*, 710–716.
52. Van Winckel, H.; Oudmaijer, R.D.; Trams, N.R. HD 133656: A new high-latitude supergiant. *Astron. Astrophys.* **1996**, *312*, 553–559.
53. Van Winckel, H.; Reyniers, M. A homogeneous study of the *s*-Process in the 21 micron carbon-rich post-AGB objects. *Astron. Astrophys.* **2000**, *354*, 135–149.
54. Rao, S.S.; Giridhar, S.; Lambert, D.L. Chemical composition of a sample of candidate post-asymptotic giant branch stars. *Mon. Not. R. Astron. Soc.* **2012**, *419*, 1254–1270. [[CrossRef](#)]
55. De Smedt, K.; Van Winckel, H.; Kamath, D.; Siess, L.; Goriely, S.; Karakas, A.I.; Manick, R. Detailed homogeneous abundance studies of 14 Galactic *s*-Process enriched post-AGB stars: In search of lead (Pb). *Astron. Astrophys.* **2016**, *587*, A6. [[CrossRef](#)]
56. Kwok, S.; Volk, K.M.; Hrivnak, B.J. A 21 micron emission feature in four proto-planetary nebulae. *Astrophys. J.* **1989**, *345*, L51–L54. [[CrossRef](#)]
57. Volk, K.; Sloan, G.C.; Kraemer, K.E. The 21 μm and 30 μm emission features in carbon-rich objects. *Astrophys. Space Sci.* **2020**, *365*, 88. [[CrossRef](#)]
58. Alcock, C.; Allsman, R.A.; Alves, D.R.; Axelrod, T.S.; Becker, A.; Bennett, D.P.; Cook, K.H.; Freeman, K.C.; Griest, K.; Lawson, W.A.; et al. The MACHO Project LMC Variable Star Inventory. VII. The Discovery of RV Tauri Stars and New Type II Cepheids in the Large Magellanic Cloud. *Astron. J.* **1998**, *115*, 1921–1933. [[CrossRef](#)]
59. Meixner, M.; Gordon, K.D.; Indebetouw, R.; Hora, J.L.; Whitney, B.; Blum, R.; Reach, W.; Bernard, J.; Meade, M.; Babler, B.; et al. Spitzer Survey of the Large Magellanic Cloud: Surveying the Agents of a Galaxy’s Evolution (SAGE). I. Overview and Initial Results. *Astron. J.* **2006**, *132*, 2268–2288. [[CrossRef](#)]
60. Bolatto, A.D.; Simon, J.D.; Stanimirović, S.; van Loon, J.T.; Shah, R.Y.; Venn, K.; Leroy, A.K.; Sandstrom, K.; Jackson, J.M.; Israel, F.P.; et al. The Spitzer Survey of the Small Magellanic Cloud: S³MC Imaging and Photometry in the Mid- and Far-Infrared Wave Bands. *Astrophys. J.* **2007**, *655*, 212–232. [[CrossRef](#)]
61. Gordon, K.D.; Meixner, M.; Meade, M.R.; Whitney, B.; Engelbracht, C.; Bot, C.; Boyer, M.L.; Lawton, B.; Sewilo, M.; Babler, B.; et al. Surveying the Agents of Galaxy Evolution in the Tidally Stripped, Low Metallicity Small Magellanic Cloud (SAGE-SMC). I. Overview. *Astron. J.* **2011**, *142*, 102. [[CrossRef](#)]
62. Reyniers, M.; Van Winckel, H.; Biémont, E.; Quinet, P. Cerium: The lithium substitute in post-AGB stars. *Astron. Astrophys.* **2002**, *395*, L35–L38. [[CrossRef](#)]
63. Goriely, S.; Mowlavi, N. Neutron-capture nucleosynthesis in AGB stars. *Astron. Astrophys.* **2000**, *362*, 599–614.
64. Lugaro, M.; Karakas, A.I.; Stancliffe, R.J.; Rijs, C. The *s*-Process in Asymptotic Giant Branch Stars of Low Metallicity and the Composition of Carbon-enhanced Metal-poor Stars. *Astrophys. J.* **2012**, *747*, 2. [[CrossRef](#)]
65. De Smedt, K. The Chemical Diversity of Post-AGB Stars in the Galaxy and the Magellanic Clouds. Ph.D. Thesis, Institute of Astronomy, KU Leuven, Leuven, Belgium, 2015.
66. Van Eck, S.; Goriely, S.; Jorissen, A.; Plez, B. Discovery of three lead-rich stars. *Nature* **2001**, *412*, 793–795. [[CrossRef](#)] [[PubMed](#)]
67. Masseron, T.; Johnson, J.A.; Plez, B.; van Eck, S.; Primas, F.; Goriely, S.; Jorissen, A. A holistic approach to carbon-enhanced metal-poor stars. *Astron. Astrophys.* **2010**, *509*, A93. [[CrossRef](#)]
68. Cowan, J.J.; Rose, W.K. Production of ¹⁴C and neutrons in red giants. *Astrophys. J.* **1977**, *212*, 149–158. [[CrossRef](#)]
69. Hampel, M.; Stancliffe, R.J.; Lugaro, M.; Meyer, B.S. The Intermediate Neutron-capture Process and Carbon-enhanced Metal-poor Stars. *Astrophys. J.* **2016**, *831*, 171. [[CrossRef](#)]

70. Hampel, M.; Karakas, A.I.; Stancliffe, R.J.; Meyer, B.S.; Lugaro, M. Learning about the Intermediate Neutron-capture Process from Lead Abundances. *Astrophys. J.* **2019**, *887*, 11. [[CrossRef](#)]
71. Karinkuzhi, D.; Van Eck, S.; Goriely, S.; Siess, L.; Jorissen, A.; Merle, T.; Escorza, A.; Masseron, T. Low-mass low-metallicity AGB stars as an efficient i-process site explaining CEMP-rs stars. *Astron. Astrophys.* **2021**, *645*, A61. [[CrossRef](#)]
72. Lugaro, M.; Campbell, S.W.; Van Winckel, H.; De Smedt, K.; Karakas, A.I.; Käppeler, F. Post-AGB stars in the Magellanic Clouds and neutron-capture processes in AGB stars. *Astron. Astrophys.* **2015**, *583*, A77. [[CrossRef](#)]
73. Busso, M.; Vescovi, D.; Palmerini, S.; Cristallo, S.; Antonuccio-Delogu, V. s-Processing in AGB Stars Revisited. III. Neutron Captures from MHD Mixing at Different Metallicities and Observational Constraints. *Astrophys. J.* **2021**, *908*, 55. [[CrossRef](#)]
74. Goriely, S.; Siess, L.; Choplin, A. The intermediate neutron capture process. II. Nuclear uncertainties. *Astron. Astrophys.* **2021**, *654*, A129. [[CrossRef](#)]